The performance of a polymaleic-based polymeric scale inhibitor on CaCO$_3$ inhibition under different water quality variables

Liang-Chen Wang[a,b,*], Qiao-Ling Zhang[a], Lu Wang[b,c], Liang-Bi Wang[b,c], Xiao-Jian Wang[a], Xue-Song Ju[a], Kai Cui[a], Chen-Guo Zhu[a]

[a]*School of Chemical Engineering, Lanzhou Jiaotong University, 88 West Anning Road, Lanzhou 730070, China,*
Tel./Fax: +86 931 4956556; email: lcwang1967@163.com (L.-C. Wang)
[b]*Key Laboratory of Railway Vehicle Thermal Engineering, Lanzhou Jiaotong University, Ministry of Education of China,*
88 West Anning Road, Lanzhou 730070, China
[c]*Department of Mechanical Engineering, Lanzhou Jiaotong University, 88 West Anning Road, Lanzhou 730070, China*

ABSTRACT

To investigate the performance of a polymaleic-based polymeric scale inhibitor against CaCO$_3$ scale under different water quality, hydrolyzed polymaleic acid (HPMA) is used. The influences of ions (Mg^{2+}, SO$_4^{2-}$, PO$_4^{3-}$, SiO$_3^{2-}$, Cl$^-$ and H$^+$) on the performance of HPMA against CaCO$_3$ scale are investigated by conducting static test. The effect of the mass ratio (β = [HPMA]/[CaCO$_3$]) on the performance of HPMA against CaCO$_3$ scale is also studied. The effect of HPMA on the crystals of CaCO$_3$ is examined using scanning electron microscopy (SEM). The results can be summarized as follows: the effect of β on the performance of HPMA against CaCO$_3$ scale mainly depends on CaCO$_3$ concentration; the presence of Mg^{2+}, SO$_4^{2-}$, PO$_4^{3-}$ and SiO$_3^{2-}$ can change adsorption equilibrium of carboxyl ion of HPMA onto the CaCO$_3$ crystal growth sites; both SO$_4^{2-}$ and SiO$_3^{2-}$ can enhance the performance of HPMA, but SiO$_3^{2-}$ causes performance declining in the presence of PO$_4^{3-}$; the presence of PO$_4^{3-}$ and Mg^{2+} may weaken the performance; Cl$^-$ can improve the performance and this effect increases with increasing Cl$^-$ concentration; pH value has a remarkable influence on the performance; SEM morphologies of CaCO$_3$ scale are distorted with dosage of HPMA; Ca–HPMA formation is confirmed using Fourier transform infrared spectra.

Keywords: Hydrolysis polymaleic acid; Static test; Water quality; Calcium carbonate scale; Recirculation cooling water

1. Introduction

With the development of industry, agriculture and urbanization, the demand for water is growing continuously in China [1]. For the purpose of saving water, the concentration ratio of recirculation cooling water increases obviously in recent years. As a result, the electrolyte concentration of recirculation cooling water increases remarkably, and the risk of corrosion, scaling and microbiological growth increases unavoidably. To retard scaling, inhibitors are widely used in industry. Being an efficient scale inhibitor, polymer scale inhibitors containing the carboxylic acid group in their molecules have become highly promising in water treatment fields. For instance, hydrolyzed polymaleic anhydride (HPMA) is successfully used as a scale inhibitor in water treatment fields [2]; the performance of polyacrylic acid is largely dependent on the product purity and the molecular weight; poly(aspartic acid), polyepoxysuccinic acid and carboxymethyl inulin, as three typical representatives of green inhibitor, are being used increasingly in water treatment plants [3–7]. However, owing to the complexity of water quality, the performance of these polymers will be weakened largely in the actual use [8,9]. For example, these polymers can form salts with alkaline earth metal ions in the water, which may be limiting the efficiency of these polymer scale inhibitors [10,11].

* Corresponding author.

Table 1 shows the water quality of a petrochemical plant in China. As shown in Table 1, the change of water quality mainly focuses on the ion concentration and the concentration ratio: Ca^{2+} concentration changes from 146 to 730 mg/L and its concentration ratio is 5, but PO_4^{3-} concentration increases from 4.3 to 5 mg/L and its concentration ratio is about 1, while SiO_2 concentration rises from 4.7 to 15 mg/L and its concentration ratio is about 3.2. These suggest that SiO_2 scale and $Ca_3(PO_4)_2$ scale deposit in the concentrated process. In this case, solubility product of calcium carbonate is $[Ca^{2+}] \times [CO_3^{2-}] = (0.73/40) \times (0.026/60) = 5.48 \times 10^{-6} \gg K_{so}$ ($K_{so} = 1.58 \times 10^{-9}$, the effect of ionic strength is ignored), and solubility product of calcium sulfate is $[Ca^{2+}] \times [SO_4^{2-}] = (0.73/40) \times (0.6/96) = 11.4 \times 10^{-5} > K_{so}$ ($K_{so} = 2.57 \times 10^{-5}$, the effect of ionic strength is ignored), it is obvious that the tendency of Ca^{2+} and CO_3^{2-} to form $CaCO_3$ scale is far greater than that of Ca^{2+} and SO_4^{2-} to form $CaSO_4$ scale in the recirculation cooling water. Therefore, in this study, calcium carbonate is the predominant component of tenacious scale.

Formation of $CaCO_3$ scale is highly depended on the water quality and operating conditions. A large number of studies are reported in literature dealing with the effects of the water quality on $CaCO_3$ scale in the presence of scale inhibitors. For instance, Can and Üner [12] studied the performance of poly(maleic anhydride-alt-acrylic acid) inhibiting against $CaCO_3$ scale with total calcium increasing from 500 to 1,200 ppm, the inhibition performance of copolymer against $CaCO_3$ scale increases with the raise of calcium concentration. Guo et al. [13] synthesized a scale inhibitor copolymer with maleic anhydride, styrene sulfonic sodium, acrylic amide and chitosan in the laboratory, the inhibition performance of the copolymer against $CaCO_3$ scale increases first and then decreases with both Ca^{2+} and CO_3^{2-} concentrations increasing from 0.003 to 0.009 mol/L. Kan et al. [14] investigated the mechanism of nitrilotris (methylene phosphonic acid) (H6NTMP)/calcite reaction, the reaction of phosphonate with calcite can be described as a Langmuir isotherm at low phosphonate concentration,

but phosphonate cannot cover the full calcite surface at saturation, while Ca2.5HNTMP forms at higher phosphonate concentration. Demadis and Katarachia [15] investigated the crystallization and structure of a Ca–AMP complex salt. They found that at higher pH regimes AMP (amino-tris-methylene phosphonate) undergoes further deprotonation resulting in an increase in its effective negative charge. AMP complexation with Ca^{2+} will require a larger number of Ca^{2+} ions to achieve neutrality. Yan et al. [10] studied the adsorption and precipitation of diethylenetriamine penta (methylene phosphonic acid) (DTPMP) and phosphino-polycarboxylic acid on Eagle Ford and Marcellus Shales, they found that surface adsorption occurs on both Eagle Ford and Marcellus Shales at low DTPMP concentration, but DTPMP and calcium can form precipitate on Eagle Ford above certain concentration. Jonasson et al. [16] found that a calcium diethylenetriamine-penta (methylene phosphonate) solid phase is uniformly distributed on calcite surface at low phosphonate concentrations, but when phosphonate concentration is high enough, an intimate mixture of calcite and calcium phosphonate precipitates is observed. Gill [17] proposed that silica scale will form onto the $CaCO_3$ precipitated when the hard scale crystal matrix is provided by the $CaCO_3$ precipitated and this crystal matrix can be captured by SiO_2. He also found that when $CaCO_3$ or other mineral scales are fully suppressed, SiO_2 concentration in water is usually higher than that scales without effectively controlled. Chen et al. [18] found that Mg^{2+} can be adsorbed onto the deposited crystals and the ratio of Mg^{2+} in the deposition is proportional to the ratio of Mg/Ca in the scaling water. Eriksson et al. [19] proposed that the electrokinetic charge and the dissolution of the calcite are a function of the concentration of anionic polyelectrolyte with NaCl concentration ranging 0.001–0.5 mol/L, the zeta potential of calcite increases with NaCl concentration at low sodium polyacrylate (NaPA) concentration ([NaPA] < 0.5% of calcite content).

In summary, although the influence of the water quality on $CaCO_3$ scale in the presence of scale inhibitors are investigated intensively, and some very important results are obtained with the artificial water, significant gaps still exist in our understanding of the effect of the real water quality on the performance of scale inhibitors against $CaCO_3$ scale because the real water quality (as shown in Table 1) is totally different from cooling water used in above mentioned studies. There are a few reports focused on studying the effects of the real water quality on the performance of scale inhibitors. Furthermore, for most of the polymer scale inhibitors used in the open recirculation cooling water system, owing to the proprietary and the patented nature, a systematic and scientific approach for their working behavior is scarce and hence the impact of the water quality on the performance of polymer scale inhibitors is still lacking.

Motivated by the facts mentioned above, HPMA is used as a sample of a polymaleic-based polymeric scale inhibitor to investigate the effects of the water quality on the performance of scale inhibitors against $CaCO_3$ scale by conducting static test. The cooling water is prepared artificially according to the data illustrated in Table 1. The influence of ions on the performance of HPMA mainly includes Mg^{2+}, SO_4^{2-}, PO_4^{3-}, SiO_3^{2-}, Cl^- and H^+. The effects of the mass ratio ($\beta = [HPMA]/[CaCO_3]$) and the influence of ions on the performance of

Table 1
Water quality of a petrochemical plant in China (25°C)

Parameter	Cooling water	Fresh water
Ca^{2+}, mg/L	730	146
Mg^{2+}, mg/L	55	–
Cl^-, mg/L	270	45
HCO_3^-, mg/L	140	–
CO_3^{2-}, mg/L	20	–
SO_4^{2-}, mg/L	600	–
SiO_2, mg/L	15	4.7
Total iron, mg/L	0.7	–
Dissolved oxygen, mg/L	9	–
Orthophosphate, mg/L	5	–
pH	8.3	8.4
Hardness (CaO), mg/L	1,150	230
Cycles of concentration	5	–
Heterotrophic bacteria	1,900	–
Total base, mg/L	170	150

HPMA against CaCO₃ scale are studied. The effects of HPMA concentrations on the morphology of CaCO₃ deposition under static test conditions are investigated using scanning electron microscopy (SEM).

2. Experimental

2.1. The experimental system

The static test is conducted as the method reported by Shen et al. [20]. The test solution is mainly composed of Ca^{2+}, HCO_3^-, CO_3^{2-} and the other ions (such as Mg^{2+}, SO_4^{2-}, PO_4^{3-}, SiO_3^{2-}, Cl^- and H^+). The concentration range of the other ions is: $[PO_4^{3-}]$ = 4–7 mg/L, $[SO_4^{2-}]$ = 400–700 mg/L, $[Mg^{2+}]$ = 15–60 mg/L, $[SiO_3^{2-}]$ = 5–20 mg/L and $[Cl^-]$ = 100–310 mg/L. The test solutions are maintained at 80°C for 10 h in water bath. The remaining Ca^{2+} is titrated by ethylenediaminetetraacetic acid (EDTA) standard solution. The inhibition efficiency, η, is defined as [21]:

$$\eta = \frac{V_2 - V_1}{V_0 - V_1} \times 100\%$$

where V_0 is the volume of EDTA without HPMA at the starting, V_1 is the volume of EDTA without HPMA after incubation and V_2 is the volume of EDTA with HPMA after incubation.

2.2. Chemicals and reagents

EDTA, calcium nitrate, sodium silicate, sodium bicarbonate, sodium carbonate, sodium hydroxide, sodium chloride, hydrochloric acid, magnesium nitrate, sodium sulfate and sodium phosphate are analytical grade and supplied by Tianjin Benchmark Chemical Reagent Co., Ltd., Tianjin, P.R. China. Commercial grade HPMA (MW = 480, the degree of polymerization is 2, and solid content is 25%) is supplied by Shandong Taihe Water Treatment Technologies Co., Ltd., China (Shandong province, P.R. China).

3. Results and discussion

3.1. Effect of β on HPMA inhibition against CaCO₃ scale in different CaCO₃ concentrations

CaCO₃ concentration of the test solution is controlled as follows: 200, 300, 400, 500, 600, 800, 1,000 and 1,200 mg/L, respectively. The mass ratio (β = [HPMA]/[CaCO₃]) ranges from 0.008 to 0.056 for every test solution. The test solution is maintained at 80°C for 10 h in water bath. Fig. 1 shows the effect of β on the performance of HPMA against CaCO₃ scale. It can be seen that eight curves of the inhibition efficiency present with the same trend: the inhibition efficiency increases steadily with the raise of β from 0.008 to 0.024, and then it presents a decrease with β increasing from 0.024 to 0.056; it is notable that the inhibition efficiency has reached the maximum value when β = 0.024, which is independent on CaCO₃ concentration; moreover, the inhibition efficiency decreases with increasing CaCO₃ concentration from 300 to 1,200 mg/L at the same β, it is clear that the performance of HPMA against CaCO₃ scale is deteriorated with the increase of CaCO₃ concentration. But the change in the inhibition efficiency highly depends on CaCO₃ concentration: for 200 mg/L,
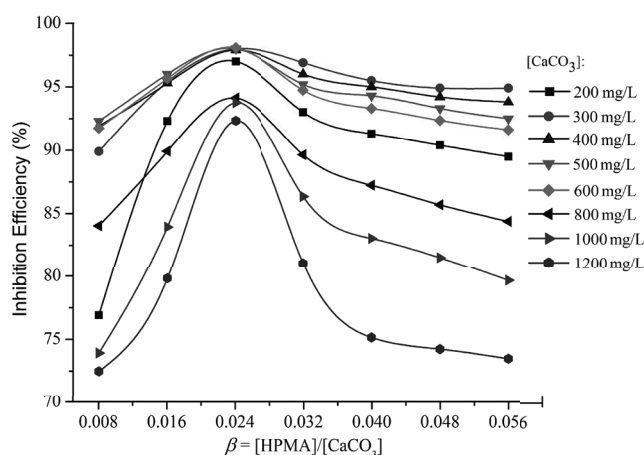
Fig. 1. The influence of β on HPMA inhibition against CaCO₃ scale under the static test conditions.

Δη = 94%–77% = 17%; for 300–600 mg/L, Δη = 97%–90% = 7%; for 800 mg/L, Δη = 93%–84% = 9%; for 1,000 mg/L, Δη = 93%–74% = 19%; for 1,200 mg/L, Δη = 92%–72% = 20%. These indicate that the effect of β on the performance of HPMA is not obvious for 300–600 mg/L, but it is becoming more significant with increasing CaCO₃ concentration from 800 to 1,200 mg/L.

The increase in the inhibition efficiency is due to more CaCO₃ crystals stabilized in the bulk solution with an increase in dosage of HPMA; but the maximum inhibition efficiency is related to adsorption equilibrium owing to carboxylic ion of HPMA adsorbing onto CaCO₃ crystal surface at 80°C, in this case the interactions between HPMA and CaCO₃ crystal, HPMA and water, water and CaCO₃ crystal, and HPMA and HPMA have reached a certain balance; while the decrease in the inhibition efficiency may be contributed to agglomeration of the dispersed CaCO₃ crystal and Ca–HPMA formation [10,11].

3.2. Effect of SO₄²⁻ on HPMA inhibition against CaCO₃ scale

The test solution consists mainly of Ca^{2+} (730 mg/L), HCO_3^- (180 mg/L), CO_3^{2-} (26 mg/L) and SO_4^{2-} (400–700 mg/L). β (β = [HPMA]/400) ranges from 0.008 to 0.056 for every test solutions. The test solutions are maintained at 80°C for 10 h in water bath. In the presence of SO_4^{2-}, four curves of the inhibition efficiency with same trend are illustrated in Fig. 2, the inhibition efficiency increases steadily to reach the maximum and followed by a continuous decrease as β increases. But the change in the inhibition efficiency actually depends on SO_4^{2-} concentration: for 400 mg/L, Δη = 92%–77% = 15%; for 500 mg/L, Δη = 95%–84% = 11%; for 600 mg/L, Δη = 96%–86% = 10%; for 700 mg/L, Δη = 97%–92% = 5% but for 0 mg/L, Δη = 98%–79% = 19%. It is obvious that the change reduces with the raise of SO_4^{2-} concentration for β ranging 0.008–0.056, implying that the effect of β on the performance of HPMA decrease with increasing SO_4^{2-} concentration. In fact this change is due to the following reasons: the first is the competitive adsorption between SO_4^{2-} and carboxyl ion of HPMA onto the CaCO₃ crystal growth sites, retarding the growth of CaCO₃ crystals; the second is the critical super saturation of CaCO₃ in the presence of SO_4^{2-} becomes higher
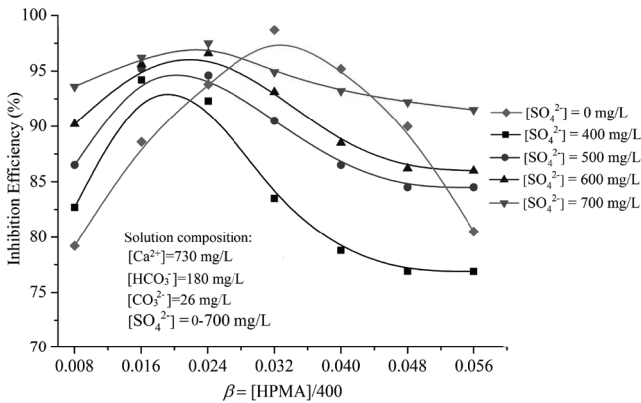
Fig. 2. The influence of SO_4^{2+} on HPMA inhibition against $CaCO_3$ scale.

Fig. 3. The influence of PO_4^{3-} on HPMA inhibition against $CaCO_3$ scale.

than that in the absence of SO_4^{2-} [22]. Additionally, the maximum inhibition efficiency (η_{max}) is related to adsorption equilibrium owing to carboxylic ion and SO_4^{2-} adsorbing onto $CaCO_3$ crystal surfaces at 80°C for different SO_4^{2-} concentrations, η_{max} is highly dependent upon SO_4^{2-} concentration: for 400 mg/L, η_{max} = 92% at β = 0.019; for 500 mg/L, η_{max} = 94% at β = 0.021; for 600 mg/L, η_{max} = 96% at β = 0.023; for 700 mg/L, η_{max} = 97% at β = 0.024; but for 0 mg/L, η_{max} = 98% at β = 0.032. These indicate that β corresponding to η_{max} increases with the raise of SO_4^{2-} concentration as well as η_{max}, which suggests that the presence of SO_4^{2-} will accelerate adsorption equilibrium and adsorption equilibrium moves to low dosage of HPMA. However the reduction in the inhibition efficiency is probably contributed to co-deposition of $CaCO_3$ and $CaSO_4$ scales at high β. The presence of SO_4^{2-} seems to promote this process and this effect decreases with increasing SO_4^{2-} concentration [23,24].

On the other hand, the inhibition efficiency increases with the raise of SO_4^{2-} concentration at the same β, which means that the presence of SO_4^{2-} can enhance the performance of HPMA against $CaCO_3$ scale, and this enhancement increases with the raise of SO_4^{2-} concentration. The enhancement is attributed to more $CaCO_3$ crystal growth sites adsorbed by SO_4^{2-} ion than by carboxyl ion of HPMA with the raise of SO_4^{2-} concentration, and at the same time the critical super saturation of $CaCO_3$ will increase with the raise of SO_4^{2-} concentration [25,26].

3.3. Influence of PO_4^{3-} ion on HPMA inhibition against $CaCO_3$ scale

The test solution is mainly composed of Ca^{2+} (730 mg/L), HCO_3^- (180 mg/L), CO_3^{2-} (26 mg/L) and PO_4^{3-} (4–7 mg/L). β (β = [HPMA]/400) ranges from 0.008 to 0.056 for every test solution. The test solutions are maintained at 80°C for 10 h in water bath. Fig. 3 shows the effect of PO_4^{3-} on HPMA against $CaCO_3$ scale. For the same solution, the inhibition efficiency increases continuously to reach the maximum (the increase stage) and then decreases steadily (the reduction stage) as β increases. The increase stage highly depends on PO_4^{3-} concentration: for 4 mg/L, $\Delta\eta$ = 92%–86% = 6%, $\Delta\beta$ = 0.016, $(\Delta\eta)/(\Delta\beta)$ = 3.75; for 5 mg/L, $\Delta\eta$ = 93%–86% = 7%, $\Delta\beta$ = 0.016, $(\Delta\eta)/(\Delta\beta)$ = 4.375; for 6 mg/L, $\Delta\eta$ = 92%–81% = 11%,
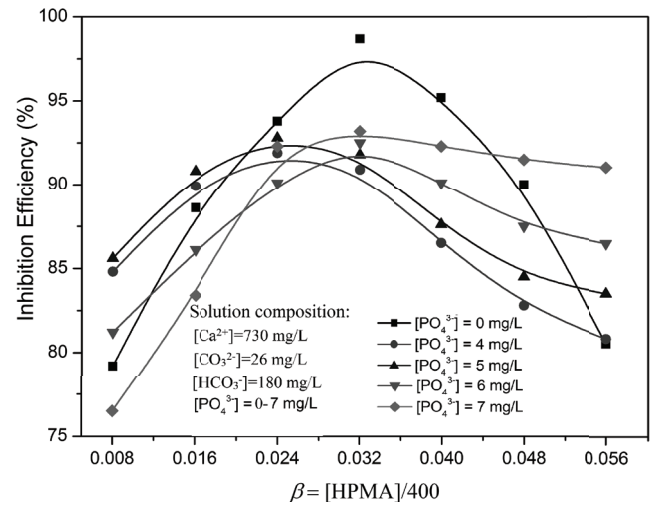
$\Delta\beta$ = 0.024, $(\Delta\eta)/(\Delta\beta)$ = 4.583 and for 7 mg/L, $\Delta\eta$ = 93%–77% = 16%, $\Delta\beta$ = 0.024, $(\Delta\eta)/(\Delta\beta)$ = 6.666. It is clear that the effect of β on the performance of HPMA increases with increasing PO_4^{3-} concentration. The maximum efficiency (η_{max}) also relies on PO_4^{3-} concentration: for 4 mg/L, η_{max} = 92% at β = 0.024; for 5 mg/L, η_{max} = 93% at β = 0.024; for 6 mg/L, η_{max} = 92% at β = 0.032; for 7 mg/L, η_{max} = 93% at β = 0.032. Obviously, η_{max} in the absence of PO_4^{3-} is bigger than that in the presence of PO_4^{3-}, the presence of PO_4^{3-} can change the adsorption equilibrium of carboxylic ion of HPMA onto $CaCO_3$ crystal surfaces. Furthermore, the reduction stage largely related to PO_4^{3-} concentration: for 4 mg/L, $\Delta\eta$ = 92%–81% = 11%, $\Delta\beta$ = 0.032, $(\Delta\eta)/(\Delta\beta)$ = 3.438; for 5 mg/L, $\Delta\eta$ = 93%–84% = 9%, $\Delta\beta$ = 0.032, $(\Delta\eta)/(\Delta\beta)$ = 2.812; for 6 mg/L, $\Delta\eta$ = 92%–87% = 5%, $\Delta\beta$ = 0.024, $(\Delta\eta)/(\Delta\beta)$ = 2.08 and for 7 mg/L, $\Delta\eta$ = 93%–91% = 2%, $\Delta\beta$ = 0.024, $(\Delta\eta)/(\Delta\beta)$ = 0.833. These reveal that the effect of β on the performance of HPMA decreases with increasing PO_4^{3-} concentration. On the whole, the presence of PO_4^{3-} can weaken the performance of HPMA and this effect actually depends on the concentration of PO_4^{3-} and HPMA.

There is a chemical equilibrium between PO_4^{3-} and $Ca_3(PO_4)_2$ in water, thence a competitive adsorption occurs between $Ca_3(PO_4)_2$ and carboxylic ion of HPMA onto the growth sites of calcite in water. A small amount of adsorption of $Ca_3(PO_4)_2$ onto the growth sites of calcite can make the critical super saturation of $CaCO_3$ increase [22], but as adsorption proceeds, more $Ca_3(PO_4)_2$ adsorbed onto the growth sites of the same calcite may result in depositing of calcite. This means that the ratio of $Ca_3(PO_4)_2$ vs. carboxyl ion of HPMA on the growth sites of calcite must not exceed a critical value for stabilizing calcite in the solution. Therefore, the increase in the inhibition efficiency is due to the increase in adsorption of $Ca_3(PO_4)_2$/HPMA (below the critical value) onto the growth sites of calcite with the raise of HPMA concentration; the maximum efficiency is related to the adsorption equilibrium owing to $Ca_3(PO_4)_2$/HPMA (in the critical value) adsorbing onto $CaCO_3$ crystal surfaces at 80°C; the decrease in the inhibition efficiency might be contributed to agglomeration of the dispersed $CaCO_3$ crystal and Ca–HPMA formation at high β [10,11].

3.4. Influence of Mg^{2+} ion on HPMA inhibition against $CaCO_3$ scale

The test solution is mainly composed of Ca^{2+} (730 mg/L), HCO_3^- (180 mg/L), CO_3^{2-} (26 mg/L) and Mg^{2+} (15–60 mg/L). β (β = [HPMA]/400) changes from 0.008 to 0.056 for every test solutions. The test solutions are maintained at 80°C for 10 h in water bath. Fig. 4 shows the effect of Mg^{2+} on HPMA inhibition against $CaCO_3$ scale. It can be seen that four curves of the inhibition efficiency in the presence of Mg^{2+} show the same trend: the inhibition efficiency increases steadily in two intervals such as 0.008–0.024 and 0.032–0.040, but it reduces continuously in the other intervals such as 0.024–0.032 and 0.040–0.056. Moreover, the maximum efficiency is related to Mg^{2+} concentration: for 15 mg/L, $η_{max}$ = 87% at β = 0.024; for 30 mg/L, $η_{max}$ = 86% at β = 0.024; for 45 mg/L, $η_{max}$ = 88% at β = 0.024; for 60 mg/L, $η_{max}$ = 89% at β = 0.024, but for 0 mg/L, $η_{max}$ = 98% at β = 0.032. It is clear that the presence of Mg^{2+} can change the adsorption equilibrium of carboxylic ion of HPMA onto $CaCO_3$ crystal surfaces at 80°C and adsorption equilibrium moves to low HPMA concentration. It can also be seen that the inhibition efficiency in the absence of Mg^{2+} is bigger than that in the presence of Mg^{2+}, which suggests that the presence of Mg^{2+} may weaken the performance of HPMA against $CaCO_3$ scale. On the other hand, the inhibition efficiency fluctuates with Mg^{2+} concentration: for 15 mg/L, $Δη$ = 82%–77% = 5%; for 30 mg/L, $Δη$ = 86%–80% = 6%; for 45 mg/L, $Δη$ = 88%–78% = 10% and for 60 mg/L, $Δη$ = 90%–76% = 14%. These indicate that the effect of β on the performance of HPMA increases with increasing Mg^{2+} concentration.

As mentioned above, Mg^{2+} has much more influence on $CaCO_3$ scale than that of HPMA, which is due to the competitive adsorption between HPMA and Mg^{2+}, Mg^{2+} and Ca^{2+}/CO_3^{2-}, and HPMA and CO_3^{2-} on the $CaCO_3$ crystal surface [18,27].

3.5. Effect of SiO_2 on HPMA inhibition against $CaCO_3$ scale

The test solution is mainly composed of Ca^{2+} (730 mg/L), HCO_3^- (180 mg/L), CO_3^{2-} (26 mg/L) and SiO_2 (5–20 mg/L).

β (β = [HPMA]/400) ranges from 0.008 to 0.056 for every test solution. The test solutions are maintained at 80°C for 10 h in water bath. Fig. 5(a) shows the effect of SiO_2 on HPMA inhibition against $CaCO_3$ scale without PO_4^{3-}. The inhibition efficiency in the presence of SiO_2 increases steadily to reach the maximum and then presents a slight decrease, but the inhibition efficiency in the absence of SiO_2 varies with β in a parabolic shape. Variation of the inhibition efficiency highly depends on SiO_2 concentration: for 5 mg/L, $Δη$ = 98%–93% = 6%; for 10 mg/L, $Δη$ = 97%–90% = 7%; for 15 mg/L, $Δη$ = 96%–70% = 16%; for 20 mg/L, $Δη$ = 92%–67% = 25%; but for 0 mg/L, $Δη$ = 98%–79% = 19%. These reveal that the effect of β on the performance of HPMA increases with increasing SO_4^{2-} concentration. Moreover, the maximum inhibition efficiency ($η_{max}$) is also related to the SiO_2 concentration: for 0 mg/L, $η_{max}$ = 98% at β = 0.032; for 5 mg/L, $η_{max}$ = 98% at β = 0.018; for 10 mg/L, $η_{max}$ = 97% at β = 0.018; for 15 mg/L, $η_{max}$ = 96% at β = 0.028; and for 20 mg/L, $η_{max}$ = 92% at β = 0.032. These suggest that the presence of SiO_2 might change adsorption equilibrium of carboxylic ion of HPMA onto $CaCO_3$ crystal

Fig. 4. The influence of Mg^{2+} on HPMA inhibition against $CaCO_3$ scale.
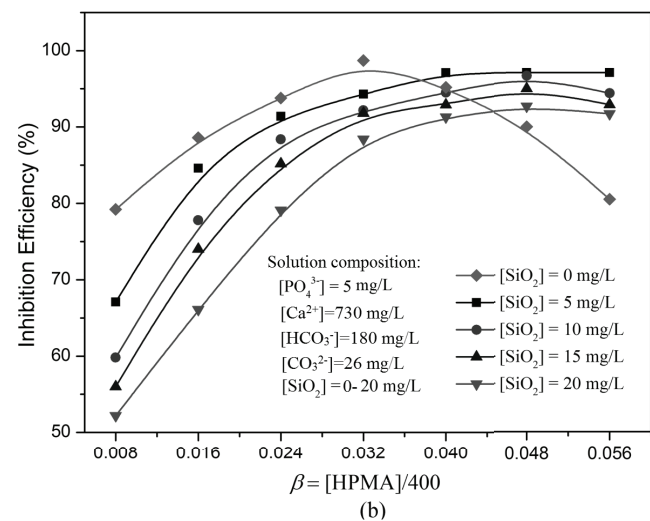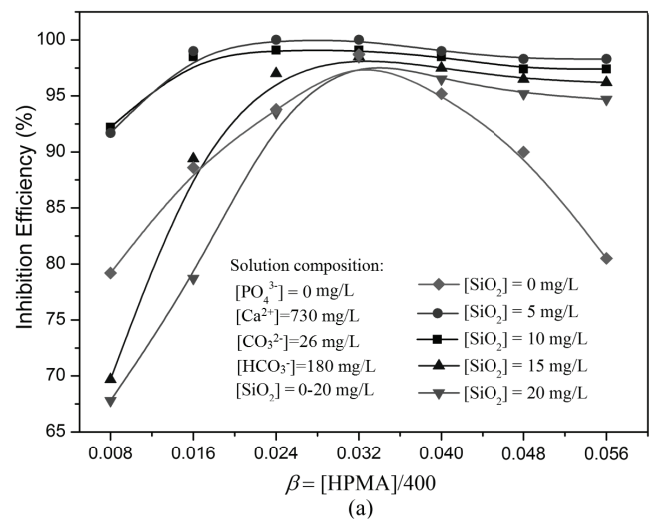
Fig. 5. The influence of SiO_2 on HPMA inhibition against $CaCO_3$ scale: (a) $[PO_4^{3-}]$ = 0 mg/L and (b) $[PO_4^{3-}]$ = 5 mg/L.

surfaces at 80°C and adsorption equilibrium moves to low dosage of HPMA. On the other hand, the inhibition efficiency decreases with the raise of SiO_2 concentration at the same β, which means that the presence of SO_4^{2-} can improve the performance of HPMA against $CaCO_3$ scale and this effect decreases with the raise of SiO_2 concentration.

There is a chemical equilibrium between SiO_3^{2-} and the silica oligomers in water, the adsorption of SiO_3^{2-} onto the growth sites of calcite can make the critical supersaturation of $CaCO_3$ increase obviously, but the adsorption of charged small silica oligomers onto the $CaCO_3$ crystal surfaces will form silica scale with increasing time [17]. Therefore, the increase in the inhibition efficiency is due to the increase in competitive adsorption of SiO_3^{2-}/HPMA onto the growth sites of calcite with the raise of HPMA concentration; but the maximum efficiency is related to the adsorption equilibrium owing to SiO_3^{2-}/HPMA adsorbing onto $CaCO_3$ crystal surfaces at 80°C; while the slight decrease in the inhibition efficiency is probably contributed to charged small silica oligomers adsorbing onto the $CaCO_3$ crystal surfaces at high β.

Fig. 5(b) shows the effect of SiO_2 on the performance of HPMA against $CaCO_3$ in the presence of PO_4^{3-}. It can be seen that four curves present with the same trend in the presence of PO_4^{3-} is similar to that in the absence of PO_4^{3-} as shown in Figs. 5(a) and (b). But for the same β and SiO_2 concentration, the inhibition efficiency in the presence of PO_4^{3-} is less than that in the absence of PO_4^{3-}, and the inhibition efficiency decreases with the raise of SiO_2 concentration for the same β, which reveal that SiO_2 can weaken the performance of HPMA against $CaCO_3$ scale in the presence of PO_4^{3-}. Furthermore, the change in the inhibition efficiency highly relies on SiO_2 concentration: for 5 mg/L, $\Delta\eta = 98\%-68\% = 30\%$; for 10 mg/L, $\Delta\eta = 96\%-60\% = 36\%$; for 15 mg/L, $\Delta\eta = 94\%-56\% = 38\%$; for 20 mg/L, $\Delta\eta = 92\%-52\% = 40\%$ but for 0 mg/L, $\Delta\eta = 98\%-79\% = 19\%$. It is obvious that the effect of β on the performance of HPMA increases with increasing SiO_2 concentration. The maximum inhibition efficiency, η_{max}, is also related to the SiO_2 concentration: for 5 mg/L, $\eta_{max} = 97\%$ at $\beta = 0.044$; for 10 mg/L, $\eta_{max} = 96\%$ at $\beta = 0.048$; for 15 mg/L, $\eta_{max} = 94\%$ at $\beta = 0.048$ and for 20 mg/L, $\eta_{max} = 93\%$ at $\beta = 0.048$. These reveal that both SiO_3^{2-} and $Ca_3(PO_4)_2$ would change the adsorption equilibrium of carboxylic ion onto $CaCO_3$ crystal surfaces at 80°C and adsorption equilibrium moves to high HPMA concentration, which is different from that in the absence of PO_4^{3-}. It is certain that the presence of $Ca_3(PO_4)_2$ and the $CaCO_3$ precipitated in the circulation cooling water might accelerate the deposition of SiO_2 scale.

Under these conditions, apart from a chemical equilibrium between SiO_3^{2-} and the silica oligomers in water, there is still another chemical equilibrium between PO_4^{3-} and $Ca_3(PO_4)_2$, the competitive adsorption of SiO_3^{2-} and/or $Ca_3(PO_4)_2$ onto the growth sites of calcite can make the critical supersaturation of $CaCO_3$ increase obviously, but the adsorption of charged small silica oligomers onto the precipitated $CaCO_3$ or $Ca_3(PO_4)_2$ will form silica scale, resulting in a rapid reduction in the inhibition efficiency.

3.6. Effect of Cl^- on HPMA inhibition against $CaCO_3$ scale

The test solution is composed of Ca^{2+} (730 mg/L), HCO_3^- (180 mg/L), CO_3^{2-} (26 mg/L), and Cl^- (100–310 mg/L).

β ($\beta = $ [HPMA]/400) ranges from 0.008 to 0.056 for every test solutions. The test solutions are maintained at 80°C for 10 h in water bath. Fig. 6 shows the effect of Cl^- on HPMA inhibition against $CaCO_3$ scale. For the same solution, the inhibition efficiency increases quickly to reach the maximum and then reduces slightly as β ranges from 0.024 to 0.056. But the inhibition efficiency varies with Cl^- concentration: for 100 mg/L, $\Delta\eta = 86\%-71\% = 15\%$; for 150 mg/L, $\Delta\eta = 90\%-76\% = 14\%$; for 200 mg/L, $\Delta\eta = 94\%-81\% = 13\%$; for 250 mg/L, $\Delta\eta = 96\%-84\% = 12\%$; for 270 mg/L, $\Delta\eta = 97\%-86\% = 11\%$; for 290 mg/L, $\Delta\eta = 99\%-90\% = 9\%$; for 310 mg/L, $\Delta\eta = 100\%-96\% = 4\%$ but for 0 mg/L, $\Delta\eta = 98\%-79\% = 19\%$. These indicate that the effect of β on the performance of HPMA decreases with increasing Cl^- concentration. Additionally, the inhibition efficiency increases with the raise of Cl^- concentration for the same β, implying that the presence of Cl^- can improve the performance of HPMA against $CaCO_3$ scale and this effect increases with the raise of Cl^- concentration. On the other hand, the maximum inhibition efficiency (η_{max}) is largely dependent upon Cl^- concentration: for 100 mg/L, $\eta_{max} = 86\%$ at $\beta = 0.038$; for 150 mg/L, $\eta_{max} = 90\%$ at $\beta = 0.035$; for 200 mg/L, $\eta_{max} = 94\%$ at $\beta = 0.025$; for 250 mg/L, $\eta_{max} = 97\%$ at $\beta = 0.024$; for 270 mg/L, $\eta_{max} = 98\%$ at $\beta = 0.023$; for 290 mg/L, $\eta_{max} = 99\%$ at $\beta = 0.022$; for 310 mg/L, $\eta_{max} = 100\%$ at $\beta = 0.020$ but for 0 mg/L, $\eta_{max} = 98\%$ at $\beta = 0.032$. It is clear that β corresponding to η_{max} decreases with the raise of Cl^- concentration, but η_{max} increases with the raise of Cl^- concentration. These indicate that the presence of Cl^- will accelerate the adsorption equilibrium and adsorption equilibrium moves to low HPMA concentration.

HPMA can inhibit against $CaCO_3$ scale efficiently through adsorption of HPMA onto crystallographic surfaces of a growing nucleus after the nucleation period. Cl^- cannot be adsorbed onto the growing nucleus, but it can increase the zeta potential of the growing nucleus [19], the increase of the zeta potential can enhance adsorption of HPMA onto the crystallographic surfaces, and the increase in the adsorption of HPMA can make the critical supersaturation of $CaCO_3$ increase remarkably [22].

3.7. Influence of pH on HPMA inhibition against $CaCO_3$ scale

The test solution is composed of Ca^{2+} (730 mg/L), HCO_3^- (180 mg/L), CO_3^{2-} (26 mg/L) and pH (7.5–9.0).
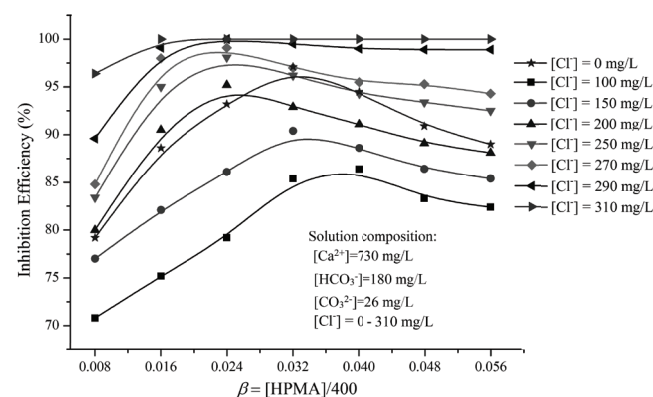
Fig. 6. The influence of Cl^- ion on HPMA inhibition against $CaCO_3$ scale.

β (β = [HPMA]/400) ranges from 0.008 to 0.056 for every test solutions. The test solutions are maintained at 80°C for 10 h in water bath. Fig. 7 shows the effect of pH on HPMA inhibition against $CaCO_3$ scale. It can be seen that the change of the inhibition efficiency is largely depended on pH value: for pH = 7.5, $\Delta\eta$ = 96%–82% = 14%; for pH = 8.0, $\Delta\eta$ = 85%–75% = 10%; for pH = 8.5, $\Delta\eta$ = 45%–10% = 35% and for pH = 9.0, $\Delta\eta$ = 25%–5% = 20%. These reveal that the performance of HPMA is very sensitive to the change of pH value, especially the inhibition efficiency reduces dramatically as pH value rises from 8.0 to 8.5, the reduction in inhibition performance is up to 50% as $\beta < 0.032$ and 35% when $\beta > 0.040$. Furthermore, the maximum inhibition efficiency, η_{max}, is related to pH value: for pH = 7.0, η_{max} = 97% at β = 0.024; for pH = 8.0, η_{max} = 85% at β = 0.032; for pH = 8.5, η_{max} = 45% at β = 0.040 and for pH = 9.0, η_{max} = 25% at β = 0.048. This indicates that β corresponding to the maximum efficiency increases with the increase in pH value, and pH might influence the adsorption equilibrium of carboxylic ion adsorbing on $CaCO_3$ crystal surface and adsorption equilibrium moves to high HPMA concentration. On the other hand, the inhibition efficiency obviously decreases with increasing pH value at the same β. A reduction in inhibition efficiency might be attributed to changes in the electric charge of $CaCO_3$ crystals and in the hydrogen bonding capability of HPMA [28]. In general, pH has a remarkable influence on HPMA inhibition against $CaCO_3$ scale, this effect can be attributed to enhancement in agglomeration and growth of the dispersed $CaCO_3$ crystal as pH value increases [10,29–32].

3.8. SEM pictures of CaCO₃ crystals with different β

The experimental condition is same as in section 3.1. The $CaCO_3$ concentration is 600 mg/L and β ranges from 0 to 0.048. The deposition of $CaCO_3$ scale on the upper surface of a cylinder is investigated using SEM, the cylinder (Ø3×4 mm) is made by 316L stainless steel and its upper surface is polished before use, the cylinder is placed in the test solutions with the polished surface upward at the beginning of the experiment [32].

Fig. 8(a) shows SEM photographs of $CaCO_3$ in the absence of HPMA. It can be seen that both rod-like aragonite and rhombohedral calcite crystals are found in the deposition [32,33]. The presence of rod-like aragonite in the deposition is owing to the run time being not enough for aragonite to transform into stable calcite.
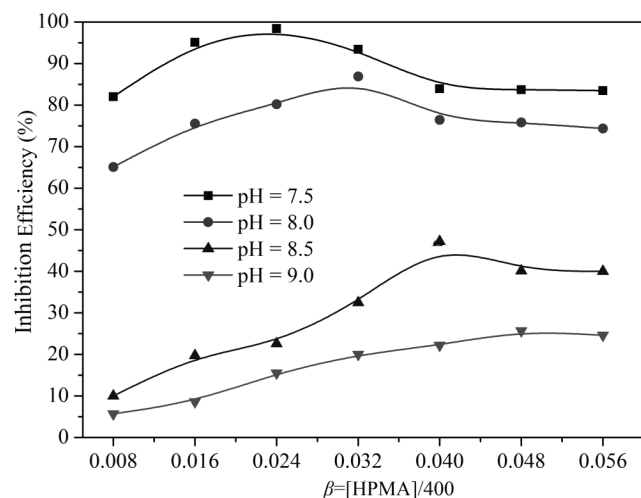
Figs. 8(b)–(f) show SEM photographs of $CaCO_3$ in the presence of HPMA. It can be seen that the structure of the deposition changes as HPMA concentration increases: as β = 0.016, Fig. 8(b) shows that the micrometric parallel growth of $CaCO_3$ crystals [34,35] are dispersed uniformly and a dense fouling layer forms on the cylinder wall, calcite crystal loses its sharp edges and acute corners, which agrees with results reported by Reddy and Hoch [36]; when β = 0.024, Fig. 8(c) shows a few micrometric parallel growth of $CaCO_3$ crystals disperse sparsely on the cylinder wall, the number of $CaCO_3$ crystal becomes few compared with Fig. 8(b), in this case HPMA may block the nucleation of $CaCO_3$ crystals and their growth; as β = 0.032, $CaCO_3$ scale is dense and has a regular shape and glossy surface as illustrated in Fig. 8(d), the formation of hard scale is related to deposition of the dispersed $CaCO_3$ crystal on the cylinder wall. When β = 0.040 and 0.048, Figs. 8(e) and (f) show massive solids with irregular shape deposit loosely on the cylinder wall, which might be attributed to co-deposition of the dispersed $CaCO_3$ crystal and Ca–HPMA precipitation.

3.9. Influence of dosage of HPMA on FTIR spectra of deposition

In order to study Ca–HPMA formation, the experimental conditions are controlled as follows: $CaCO_3$ concentration is 1,200 mg/L, β ranges from 0 to 0.300, and the test solutions are maintained at 80°C for 72 h in water bath. Flocculent precipitation is observed in all test solutions in the presence of HPMA, the amount of flocculent precipitation increases as β increases. The Fourier transform infrared spectra (FTIR) spectra of flocculent precipitation are measured and the results are illustrated in Fig. 9: absorption bands caused by the carbonate ions of $CaCO_3$ appear at 1,627, 1,473 and 856 cm⁻¹; but absorption bands at 1,573 and 1,419 cm⁻¹ can be assigned to carboxylate ion; while a weak absorption band at 864 cm⁻¹ is attributed to bending vibration of the carbonate ions (for aragonite), which gradually disappears as dosage of HPMA increases. These are contributed to Ca–HPMA formation which is favored at high dosage of HPMA and high $CaCO_3$ concentration [10,11]. However, for high $CaCO_3$ concentration, agglomeration of the dispersed $CaCO_3$ crystal and Ca–HPMA precipitation co-deposit at low dosage of HPMA.

The growth of $CaCO_3$ scale inhibited by HPMA is due to adsorption of carboxyl group in the crystal growth points of molecular. The performance of HPMA against $CaCO_3$ scale practically depends on HPMA concentration: as HPMA concentration is below its saturation concentration, the performance increases with the raise of HPMA concentration; as HPMA concentration has reached its saturation concentration, the performance is best; while when dosage of HPMA exceeds its saturation concentration, Ca–HPMA may form and co-deposit with agglomeration of the dispersed particles of $CaCO_3$ crystal. SEM analysis shows that morphologies of $CaCO_3$ scale are distorted in the presence of HPMA. Ca–HPMA formation is proved by FTIR analysis.

Fig. 7. Influence of pH on HPMA inhibition against $CaCO_3$ scale.
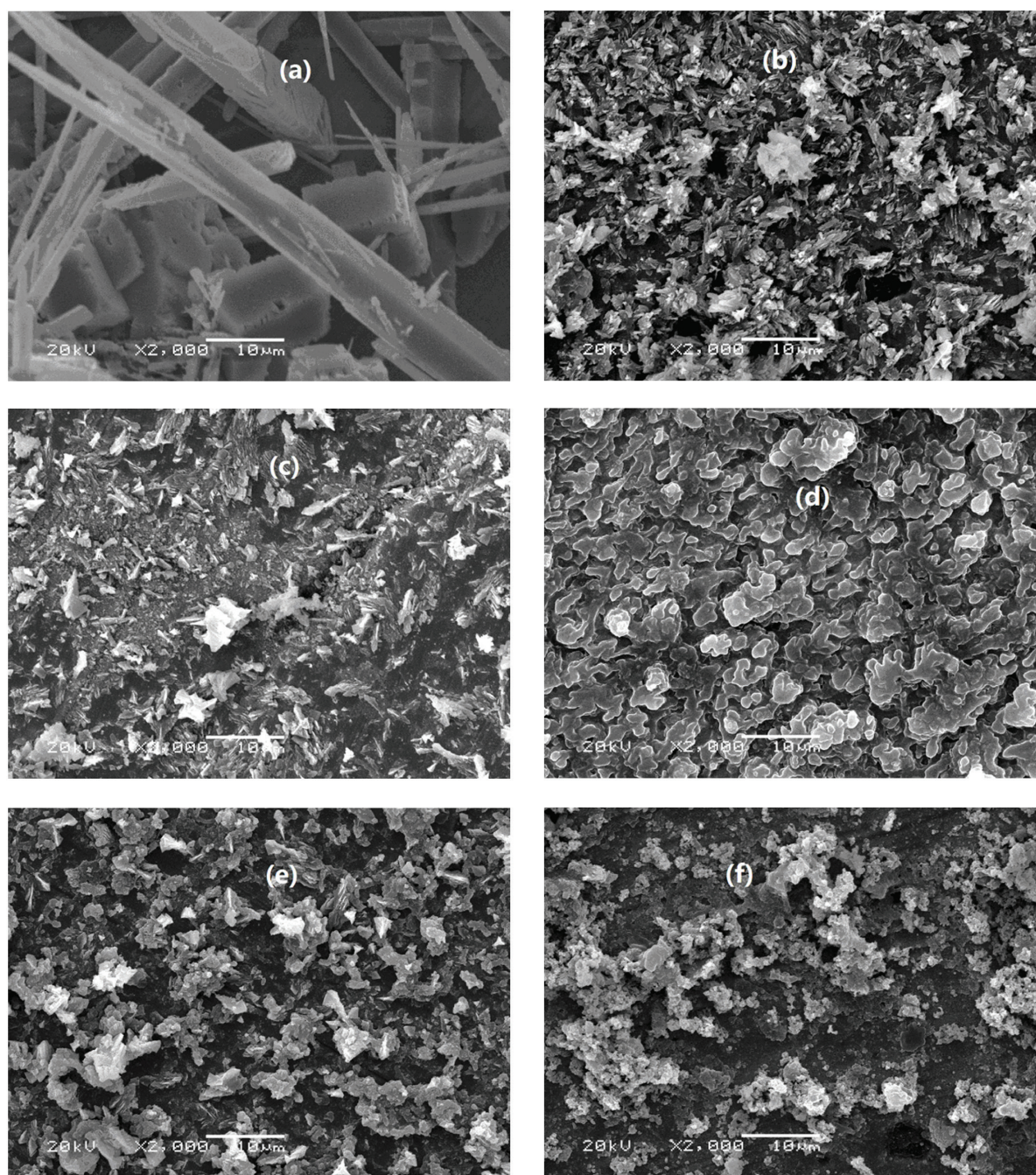
Fig. 8. SEM pictures of CaCO$_3$ precipitation: (a) $\beta = 0$, (b) $\beta = 0.016$, (c) $\beta = 0.024$, (d) $\beta = 0.032$, (e) $\beta = 0.040$ and (f) $\beta = 0.048$.

4. Conclusions

In this paper, the performance of HPMA against CaCO$_3$ scale under different water quality is investigated by conducting static tests, the water quality is based on the data gained from a real open recirculation cooling water system. The influence of HPMA on the morphology of CaCO$_3$ deposition is also investigated. The main results can be summarized as followed:

(a) The effect of β on the performance of HPMA against CaCO$_3$ scale is not obvious for 300–600 mg/L, but it is becoming more distinct with increasing CaCO$_3$ concentration from 800 to 1,200 mg/L. For the same β, the effect increases with the raise of CaCO$_3$ concentration. It is interesting that the performance of HPMA is the best when $\beta = 0.024$, which is independent on CaCO$_3$ concentration.

(b) SO$_4^{2-}$ can enhance the performance of HPMA and this enhancement increases with the raise of SO$_4^{2-}$ concentration.

(c) PO$_4^{3-}$ can weaken the performance of HPMA and this effect depends on the concentration of PO$_4^{3-}$ and HPMA.
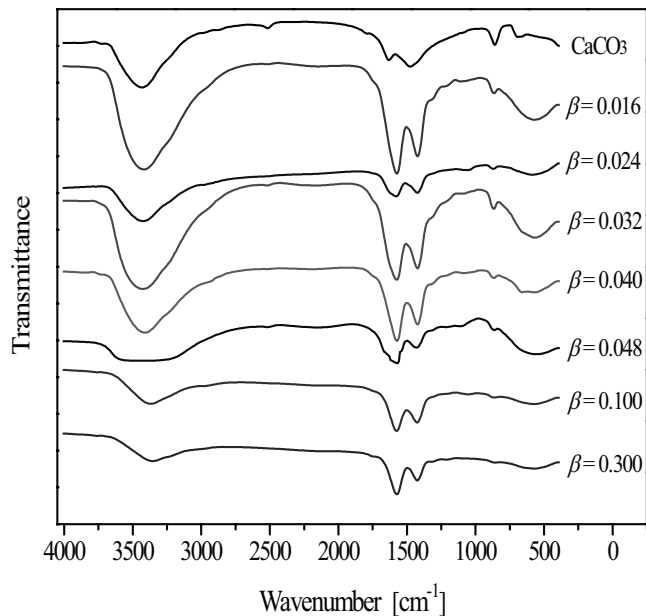
Fig. 9. FTIR spectrum of Ca–HPMA precipitation.

(d) SiO_2 can obviously promote the performance of HPMA in the absence of PO_4^{3-} and this influence decreases with the raise of SiO_2 concentration. But in the presence of PO_4^{3-}, SiO_2 may weaken the performance of HPMA and this effect increases with increasing SiO_2 concentration.

(e) Mg^{2+} can decline the performance of HPMA and keeps the performance of HPMA fluctuating in a narrow range.

(f) Cl^- can markedly improve the performance of HPMA and the effect increases with the raise of Cl^- concentration.

(g) The influence of pH on the performance of HPMA increases with increasing pH value. Especially the performance of HPMA is deteriorated remarkably as pH value increases from 8.0 to 8.5.

(h) SEM analysis shows that morphologies of $CaCO_3$ scale are distorted in the presence of HPMA. Ca–HPMA formation is proved using FTIR spectra.

Acknowledgment

References

[1] X. Zheng, D. Chen, Q. Wang, Z.X. Zhang, Seawater desalination in China: retrospect and prospect, Chem. Eng. J., 242 (2014) 404–413.

[2] P. Shakkthivel, D. Ramesh, R. Sathiyamoorthi, T. Vasudevan, Water soluble copolymers for calcium carbonate and calcium sulphate scale control in cooling water systems, J. Appl. Polym. Sci., 96 (2005) 1451–1459.

[3] S.M. Thombre, B.D. Sarwade, Synthesis and biodegradability of polyaspartic acid: a critical review, J. Macromol. Sci., 42 (2005) 1299–1315.

[4] K.D. Demadis, E. Neofotistou, E. Mavredaki, M. Tsiknakis, E.M. Sarigiannidou, S.D. Katarachia, Inorganic foulants in membrane systems: chemical control strategies and the contribution of "green chemistry", Desalination, 179 (2005) 281–295.

[5] E. Mavredaki, A. Stathoulopoulou, E. Neofotistou, K.D. Demadis, Environmentally benign chemical additives in the treatment and chemical cleaning of process water systems: implications for green chemical technology, Desalination, 210 (2007) 257–265.

[6] A. Ketsetzi, A. Stathoulopoulou, K.D. Demadis, Being "green" in chemical water treatment technologies: issues, challenges and developments, Desalination, 223 (2008) 487–493.

[7] A. Stathoulopoulou, K.D. Demadis, Enhancement of silicate solubility by use of "green" additives: linking green chemistry and chemical water treatment, Desalination 224 (2008) 223–230.

[8] K.D. Demadis, E. Mavredaki, A. Stathoulopoulou, E. Neofotistou, C. Mantzaridis, Industrial water systems: problems, challenges and solutions for the process industries, Desalination, 213 (2007) 38–46.

[9] T.A. Hoang, Mechanisms of Scale Formation and Inhibition, Mineral Scales and Deposits, Chapter 3, 2015, pp. 47–83.

[10] F. Yan, F.F. Zhang, B. Narayan, L. Wang, Z.Y. Dai, Z. Zhang, Y. Liu, G.D. Ruan, K. Amy, T. Mason, Adsorption and precipitation of scale inhibitors on shale formations, J. Pet. Sci. Eng., 13 (2015) 32–40.

[11] D.L. Verraest, J.A. Peters, H. Van Bekkum, G.M. Van Rosmalen, Carboxymethyl inulin: a new inhibitor for calcium carbonate precipitation, J. Am. Oil Chem. Soc., 73 (1996) 55–62.

[12] H.K. Can, G. Üner, Water-soluble anhydride containing alternating copolymers as scale inhibitors, Desalination, 355 (2015) 225–232.

[13] X.R. Guo, F.X. Qiu, K. Dong, X. Zhou, J. Qi, Y. Zhou, D.Y. Yang, Preparation, characterization and scale performance of scale inhibitor copolymer modification with chitosan, J. Ind. Eng. Chem., 18 (2012) 2177–2183.

[14] A.T. Kan, G.M. Fu, M.B. Tomson, Adsorption and precipitation of an aminoalkyl phosphonate onto calcite, J. Colloid Interface Sci., 281 (2005) 275–284.

[15] K.D. Demadis, S.D. Katarachia, Metal-phosphonate chemistry: synthesis, crystal, structure of calcium-aminotris-(methylene phosphonate) and inhibition of $CaCO_3$ crystal growth, Phosphorus, Sulfur Silicon Relat. Elem., 179 (2004) 627–648.

[16] R.G. Jonasson, K. Rispler, B. Wiwchar, W.D. Gunter, Effect of phosphonate inhibitors on calcite nucleation kinetics as a function of temperature using light scattering in an autoclave, Chem. Geol., 132 (1996) 215–225.

[17] J.S. Gill, Inhibition of silica-silicate deposits in industrial water, Colloids Surf., A, 74 (1993) 101–106.

[18] T. Chen, A. Neville, M.D. Yuan, Influence of Mg^{2+} on $CaCO_3$ formation-bulk precipitation and surface deposition, Chem. Eng. Sci., 61 (2006) 5318–5327.

[19] R. Eriksson, J. Merta, J.B. Rosenholm, The calcite/water interface I. Surface charge in indifferent electrolyte media and the influence of low-molecular-weight polyelectrolyte, J. Colloid Interface Sci., 313 (2007) 184–193.

[20] Z.H. Shen, J.S. Li, K. Xu, L.L. Ding, H.Q. Ren, The effect of synthesized hydrolyzed polymaleic anhydride (HPMA) on the crystal of calcium carbonate, Desalination, 284 (2012) 238–244.

[21] L.C. Wang, S.F. Li, L.B. Wang, K. Cui, Q.L. Zhang, H.B. Liu, G. Li, Relationships between the characteristics of $CaCO_3$ fouling and the flow velocity in smooth tube, Exp. Thermal Fluid Sci., 74 (2016) 143–159.

[22] N. Cabrera, D.A. Vermilyea, in: Growth and Perfection of Crystals, R.H. Doremus, B.W. Roberts, D. Turnbll, Eds., Wiley, New York, 1958, p. 313.

[23] J. Franke, A. Mersmann, The influence of the operational conditions on the precipitation process, Chem. Eng. Sci., 50 (1995) 1737–1753.

[24] Y. Zarga, H.B. Boubaker, N. Ghaffour, H. Elfil, Study of calcium carbonate and sulfate co-precipitation, Chem. Eng. Sci., 96 (2013) 33–41.

[25] R.M. Sheikholeslami, M. Ng, Calcium sulfate precipitation in the presence of non-dominant calcium carbonate: thermodynamics and kinetics, Ind. Eng. Chem. Res., 40 (2001) 3570–3578.

[26] T.H. Chong, R. Sheikholeslami, Thermodynamics and kinetics for mixed calcium carbonate and calcium sulfate precipitation, Chem. Eng. Sci., 56 (2001) 5391–5400.

[27] R.G. Compton, C.A. Brown, The inhibition of calcite dissolution/precipitation: Mg^{2+} cations, J. Colloid Interface Sci., 165 (1994) 445–449.

[28] F. Jones, A. Oliveira, A.L. Rohl, G.M. Parkinson, M.I. Ogden, M.M. Reyhani, Investigation into the effect of phosphonate inhibitors on barium sulfate precipitation, J. Cryst. Growth, 237–239 (2002) 424–429.

[29] M. Wolthers, L. Charlet, P. Van Cappellen, The surface chemistry of divalent metal carbonate minerals: a critical assessment of surface charge and potential data using the charge distribution multi-site ion complexation model, Am. J. Sci., 308 (2008) 905–941.

[30] D.W. Thompson, P.G. Pownall, Surface electrical properties of calcite, J. Colloid Interface Sci., 131 (1989) 74–82.

[31] L.F. Greenlee, F. Testa, D.F. Lawler, B.D. Freeman, P. Moulin, The effect of antiscalant addition on calcium carbonate precipitation for a simplified synthetic brackish water reverse osmosis concentrate, Water Res., 44 (2010) 2957–2969.

[32] L.C. Wang, K. Cui, L.B. Wang, H.X. Li, S.F. Li, Q.L. Zhang, H.B. Liu, The effect of ethylene oxide groups in alkyl ethoxy carboxylates on its scale inhibition performance, Desalination, 379 (2016) 75–84.

[33] S. Weiner, I. Sagi, L. Addadi, Choosing the crystallization path less traveled, Science, 309 (2005) 1027–1028.

[34] A. Kotachi, T. Miura, H. Imai, Morphological evaluation and film formation with iso-oriented calcite crystals using binary poly (acrylic acid), Chem. Mater., 16 (2004) 3191–3196.

[35] H. Imai, Mesostructured crystals: growth processes and features, Prog. Cryst. Growth Charact. Mater., 62 (2016) 212–226.

[36] M.M. Reddy, A.R. Hoch, Calcite crystal growth rate inhibition by polycarboxylic acids, J. Colloid Interface Sci., 235 (2001) 365–370.